Nanostructures

DOI: 10.1002/anie.200802744

Spontaneous Growth of Highly Conductive Two-Dimensional Single-Crystalline $TiSi_2$ Nanonets**

*Sa Zhou, Xiaohua Liu, Yongjing Lin, and Dunwei Wang**

Simple nanostructures (e.g. nanowires) form complex nanomaterials when connected by single-crystalline junctions.[1,2] These nanomaterials offer better mechanical strength and superior charge transport while preserving unique properties associated with the small-dimension nanostructure. Tremendous research interest has focused on this new class of materials, especially in the field of electronics[3] and energy applications.[4] The synthesis of these materials is challenging because of their combined features of low dimensionality and high complexity; the former requires growth suppression whereas the latter demands growth enhancement.[5] Here we report our success in growing single-crystalline two-dimensional (2D) networks of $TiSi_2$, a free-standing structure that is micrometers wide and long but only approximately 15 nm thick; beams of these networks are nanobelts $\approx$25 nm wide. This new structure can serve as a testing grounds for probing a host of intriguing properties and applications, and the synthesis should inspire work on the growth of complex nanostructures in general.

We were motivated to study $TiSi_2$ by its properties and potential applications as well as its unique crystal structures. $TiSi_2$ is an excellent electronic material as it is one of the most conductive silicides (resistivity $\approx 10\ \mu\Omega\,cm$).[6,7] $TiSi_2$ was also recently shown to be a good photocatalyst for splitting H_2O by absorbing visible light, which is a promising approach toward solar-generated H_2 as a clean energy carrier.[8] The improved charge-transport properties offered by complex nanoscale structures of $TiSi_2$ are desirable for nanoelectronics and solar energy harvesting. Their chemical synthesis is thus appealing; however, the synthetic conditions required by the two key features of complex nanostructures, low dimensionality and complexity, seem to contradict each other. Growth of one-dimensional (1D) features involves promoting additions of atoms or molecules in one direction while constraining those in all other directions; this is often achieved either by surface passivation to increase the energies of sidewall deposition (such as solution-phase synthesis) or by the introduction of impurities to lower the energies of deposition for the selected directions (most notably the vapor–liquid–solid mechanism).[9,10] Complex crystal structures, on the other hand, require controlled growth in more than one direction. The challenge in making 2D complex nanostructures is even greater as it demands more stringent controls over the complexity to limit the overall structure within two dimensions. Indeed, successful chemical syntheses of complex nanostructures have been mainly limited to 3D ones,[11–14] and demonstrations of 2D nanocrystals are less frequent. Yang et al., for instance, have reported a simple comblike ZnO nanostructure.[15] Multicrystalline nanosheets of tetragonal TiO_2 were also reported.[16,17] The complex $TiSi_2$ nanostructures of orthorhombic symmetry that we present herein represent a far more complex 2D structure than those previously achieved.

Two-dimensional $TiSi_2$ nanonets spontaneously formed as products of the simple reaction of $TiCl_4$ and SiH_4 in a H_2-rich environment at moderate temperatures ($\approx$675 °C) without any catalyst. The unique structure is shown in the scanning electron micrograph (SEM, Figure 1a). At relatively low magnifications, the high-yield products pack to resemble tree leaves, except that each sheet is composed of nanometer-scale beams (Figure 1a, inset). The structure is better seen under transmission electron microscope (TEM, Figure 1b). Within each of the 2D structures are nanobelts $\approx$25 nm wide and $\approx$15 nm thick, all linked together by single-crystalline junctions at 90° angles. To our knowledge such structures have not yet been encountered in nanomaterials; we henceforth designate them as nanonets (NNs) to emphasize the network-like characteristics.

We provide evidence that these structures are indeed two dimensional with a series of tilted TEM pictures along with analogous 2D sketches (Figure 1c–e). A similar series of tilted images was also obtained using SEM (see Figure S1 in the Supporting Information). In addition, we observed that the 2D NNs bend and roll up when pushed by a STM tip during TEM characterizations (Figure 5b); this further verifies the 2D nature and suggests that the structures are highly flexible as a result of the thinness.

High-resolution imaging and electron diffraction (ED) patterns of different regions of a representative NN reveal that the entire structure is single crystalline, including the 90° joints and the middle and ends of any given nanobelt (Figure 2). We suggest that the beams are nanobelts based on two main observations: 1) Loose ends often bend on the supporting films used for TEM, which is characteristic of nanobelts (Figure 1b);[18] and 2) the thickness of the beams in a NN ($\approx$15 nm) is obviously less than the width ($\approx$25 nm), as

[*] S. Zhou,[+] Dr. X. Liu,[+] Y. Lin, Dr. D. Wang
Department of Chemistry
Merkert Chemistry Center, Boston College
2609 Beacon Street, Chestnut Hill, MA 02467 (USA)
Fax: (+1) 617-552-2705
E-mail: dunwei.wang@bc.edu
Homepage: http://www2.bc.edu/~dwang

[+] These authors contributed equally to this work.

[**] This work was financially supported by Boston College. We are grateful to Prof. J. Kong and Y.-P. Hsieh at MIT for their generous help in carrying out Raman experiments. E. Shaw at MIT provided assistance in XPS experiments. Dr. D. Wang helped with TEM.

Supporting information for this article is available on the WWW under http://dx.doi.org/10.1002/anie.200802744.

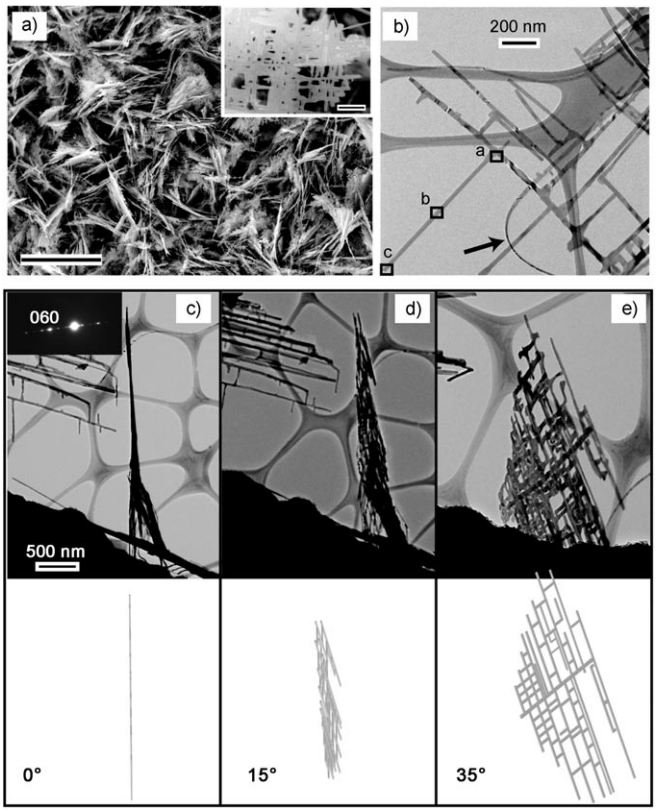

Figure 1. Electron micrographs of two-dimensional $TiSi_2$ nanonets. a) High-yield NNs pack to resemble tree leaves, with details shown in the inset at a higher magnification. Scale bars: 5 μm in main picture; 100 nm in the inset. b) A single NN viewed under TEM. All beams are connected by single-crystalline junctions at 90°. One of the beams is twisted on the bottom of the picture (arrow) and demonstrates beltlike characteristics. High-resolution TEM images of selected regions (boxes a–c) are shown in Figure 2. c–e) A series of tilted TEM pictures and corresponding schematics help to understand the structure. The electron diffraction pattern in the inset of (c) was recorded on the NN in the vertical orientation; it indicates that the NN is single crystalline and that the plane of the NN is perpendicular to the ⟨010⟩ direction (presence of strong diffraction spot of (060)).

evidenced in the tilted TEM image (Figure 1c and Figure S3 in the Supporting Information).

Further analyses of high-resolution TEM images and associated ED patterns show that the NNs have a C49 structure with the *b* axis perpendicular to the plane (Figure 1c and Figure 2a); in other words, the NNs grow primarily along the *a* and *c* directions. Using a typical NN (2 μm wide and long and 15 nm thick) as an example, the growth selectivity of different crystal directions (*a*/*b* or *c*/*b*, that is, width/thickness) is calculated to be >100. This is a remarkable value considering that no growth seeds are involved (the ends of the nanobelts within any NNs are free of impurities; Figure 2c).[19] This growth selectivity may be explained by the orthorhombic symmetry of C49 $TiSi_2$ and corresponding atomic arrangements (see Figure S4 in the Supporting Information). We speculate that Cl terminations evident in the X-ray photoelectron spectra (XPS, Figure 3d) act as a passivation layer that prevents further deposition on the *b* planes. The sidewalls of the nanobelts are likely passivated by Cl and H atoms, as well, although the terminations are less stable than those of the {010} planes.[20] When the passivation is destabilized by continuous Ti and Si deposition on the side of a beam, branching occurs. Since $TiSi_2$ preferably grows along ⟨100⟩ and ⟨001⟩, angles between connecting branches are always 90°, yielding the unique 2D network structure. It is interesting to note the phenomenon when two growing beams meet. One of the beams was observed to either change growth direction to form a 90° kink or melt into the second one to form a single-crystalline connection (Figure 3). In addition, we frequently obtained NNs composed of wider, but not thicker, nanobelts for extended growth (e.g. after a CVD time of 1 h). This implies that the {100} and {001} sides are indeed susceptible to further growth.

To further validate our hypothesized growth mechanism, we modified the growth conditions and carried out syntheses under different pressures, temperatures, and precursor gas ratios. In addition to NNs, we also obtained high-quality nanowires (NWs) (Figure 4).[21] The general trend is that lower pressure, lower $TiCl_4/SiH_4$ ratios, and higher temperatures favor NW growth while the opposite leads to more NNs.[22] Within the tested variation ranges, however, we did not observe the titanium silicide compounds reported by others.[23] Careful studies of the microstructures, however,

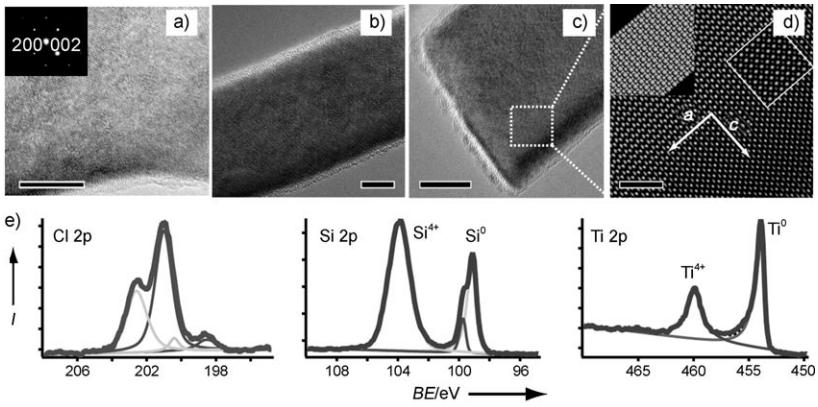

Figure 2. High-resolution TEM images of $TiSi_2$ NNs. The entire structure is single crystalline, including the joint (a), the middle (b), and the end of a nanobelt. ED pattern (inset in a) reveals that the structure is C49 $TiSi_2$. Noise reduction by iFFT in selected regions in (c) shows the Ti and Si atomic arrangements, as shown in (d), are in excellent agreement with simulated ones (white-framed inset), supporting our structural analysis. Schematic atomic arrangement viewed from ⟨010⟩ direction is also shown in the top left inset. Scale bars: 5 nm (a), 5 nm (b), 5 nm (c), and 2 nm (d). The XPS peaks of Cl, Si, and Ti with peak fittings in (e) indicate that the surface {010} planes are passivated by Cl atoms during NN growth. Composition analysis by XPS shows that the Si/Ti ratio on the surface is much greater than 2:1, substantially different from that obtained from EDS data ($\approx$1:2, see Figure S2 in the Supporting Information). This further confirms that Si content is greater on the surface and suggests Si terminations.

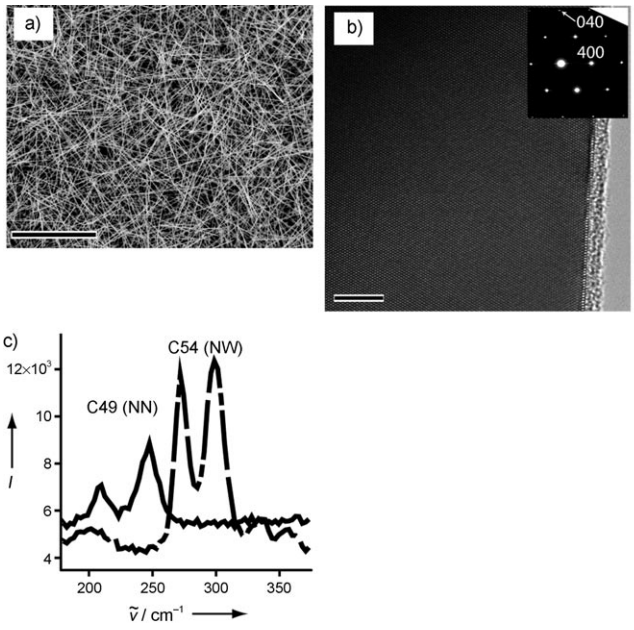

Figure 3. SEM (a) and TEM (b) images of C54 $TiSi_2$ nanowires. The microstructures are evident in the high-resolution image, ED pattern, and micro-Raman spectra (c). Scale bars: 5 μm in (a) and 5 nm in (b). $TiSi_2$ nanowires are favored for growth conditions with relatively lower Si concentrations, for example, lower pressure and higher temperature.

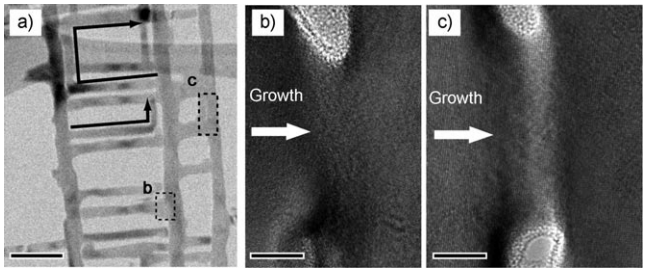

Figure 4. Kinks and melting phenomenon observed in $TiSi_2$ NN growth. When a growth front encounters an existing structure, it either changes growth direction to form 90° kinks (a) or it melts into the existing one to form a single-crystalline joint (b and c). Multiple kinks can be formed as seen in (a). Scale bars: 100 nm, 5 nm, and 5 nm (from left to right). Arrows in (b) and (c) indicate the growth direction. This observation also reaffirms the 2D nature of the growth.

revealed that although they belong to the same symmetry group (orthorhombic), NWs are C54 structures ($a = 8.236$, $b = 4.773$, $c = 8.523$ Å) and grow along the b direction. The structural difference was also confirmed by Raman spectroscopy (Figure 4c) as well as by transition electron microscopy (Figure 3b).[24,25] We suggest that relatively higher Si concentrations (afforded by higher SiH_4 ratios, higher pressures, and lower temperatures) help passivate the {010} planes of the C49 structure and therefore lead to NN growth. The degree of supersaturation of $TiSi_2$ in the gas phase may also play a role,[26] and more studies are required to reveal the details. These studies will also shed light on the growth mechanisms behind the recent syntheses of metal silicide NWs.[27,28]

For bulk $TiSi_2$, the C49 phase is reported to form first during solid-state reactions and then is converted to C54 at high temperatures (e.g. 700 °C).[29] In other words, C49 $TiSi_2$ has been regarded as the metastable phase that has higher resistivity as a result of stacking faults along the b direction. The nanostructured $TiSi_2$ synthesized here shows different properties. Not only are C49 $TiSi_2$ NNs strikingly stable—the structure is preserved after annealing in H_2 at temperatures of up to 900 °C for over 30 min—they are also highly conductive, as will be discussed later. The remarkable stability may result from the small dimensions: a film thickness of 15 nm corresponds to roughly 10–12 unit cells along ⟨010⟩ direction, within which stacking faults are unlikely events.

Complex nanostructures link low-dimensional nanomaterials by high-quality single-crystalline junctions, providing better charge transport between individual components and stronger mechanical support. They are of significant interest for nanoelectronics and emerging solar-energy harvesting. We next present the electrical properties of $TiSi_2$ NNs with a view toward potential applications. As can be seen from a typical I–V plot (Figure 5c), NNs are indeed excellent conductors.

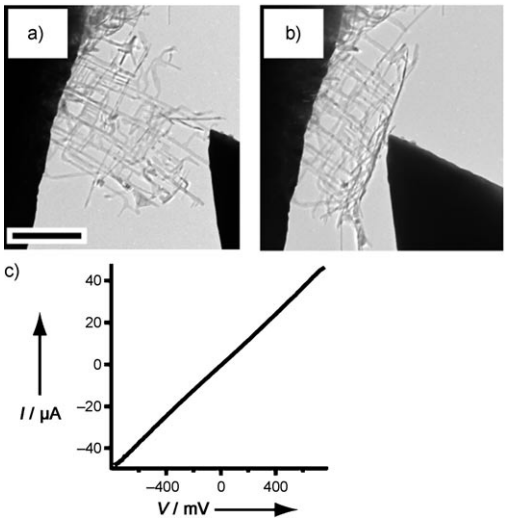

Figure 5. Electrical measurements of $TiSi_2$ NNs. The STM–TEM measurement setup is shown in (a). When pushed by the STM tip, the NN rolls up (b). The structural change is reversible, demonstrating a remarkable flexibility (the structure survives repeatable bending of curves with radii as small as < 500 nm). Scale bar: 500 nm. A typical I–V scan is plotted in (c).

Assuming a thickness of 15 nm and a width of 30 nm for a single beam within the NN, and regarding the charge transport path as the shortest distance between contacting electrodes (≈ 1 μm), we have the resistivity ≈ 10 μΩ cm; this value is in good agreement with that of bulk C54 and significantly better than that of bulk C49 $TiSi_2$. This may be explained by the absence of defects, which have been determined to be detrimental in electrical conductance in bulk C49 $TiSi_2$.

In conclusion, we have successfully synthesized a new 2D nanonet structure using simple chemical reactions. The products are high-quality single-crystalline complex struc-

tures composed of perpendicular nanobelts. The morphology was found to result from the orthorhombic crystal symmetry, and was sensitive to growth conditions: lower Si concentrations in the precursor mixture favor NW growth. The high-quality single-crystalline NNs reported here represent one of the most conductive silicides, and open the door to new exciting electronic and energy-related applications.

Experimental Section

Methods 1) Synthesis of $TiSi_2$: Chemical vapor deposition (CVD) was carried out in a homebuilt apparatus with automatic flow and pressure controls. 50 sccm (standard cubic centimeters per minute) SiH_4 (10% diluted in He) was used as the Si precursor; $TiCl_4$ vapor with an equivalent flow of 2.5 sccm was transported by 100 sccm H_2 flow. All precursors were kept at room temperature before being introduced into the reaction chamber which was heated to 675 °C. The system was kept at a constant pressure of 5 Torr during growth, and the reaction lasted 15 min. Products as dark gray powders were collected on clean Si substrates and subjected to further characterization.

2) Structural characterizations: SEM and TEM: As-grown products were characterized using scanning electron microscope (SEM, JSM 6340F) and transmission electron microscope (TEM, JEM 2010F). Energy-dispersive X-ray spectra (EDS) were collected to verify chemical compositions on both SEM and TEM samples, and comparable results (Ti/Si 1:2) were obtained. Detailed microstructures of $TiSi_2$ were carefully studied through high-resolution imaging, along with selected-area electron diffraction (SAED) patterns. For each high-resolution electron micrograph (HREM) presented in this paper, at least two SAED patterns were obtained at different zone axes to avoid indexing ambiguity. To better show the atomic arrangements in the HREMs, we performed noise reduction by inverse fast Fourier transform (iFFT). The experimental data were further compared with simulated pictures using the EMS package[30] (see Table 1 in the the Supporting Information); the resemblance was remarkable, strongly supporting the accuracy of our analyses. Raman spectroscopy: Raman spectra were recorded on a home-built Raman spectrometer at a laser excitation wavelength of 647 nm, with a power level of 1 mW and 100× object lens. X-ray photoelectron spectroscopy (XPS): XPS spectra from the $TiSi_2$ nanonets were taken with an $Al_{K\alpha}$ irradiation source (1486.69 eV) using a Kratos AXIS Ultra Imaging X-ray Photoelectron Spectrometer with 0.1 eV resolution. An internal C 1s standard was utilized to calibrate the binding energies.

3) Electrical measurements: Electrical measurements were performed in the TEM chamber using a commercial STM/TEM sample holder (Nanofactory ST1000, please see the Supporting Information for details).

Received: June 10, 2008
Published online: September 2, 2008

Keywords: chemical vapor deposition · conducting materials · electron microscopy · nanostructures

[1] L. Manna, D. J. Milliron, A. Meisel, E. C. Scher, A. P. Alivisatos, *Nat. Mater.* **2003**, *2*, 382.
[2] D. Wang, F. Qian, C. Yang, Z. H. Zhong, C. M. Lieber, *Nano Lett.* **2004**, *4*, 871.
[3] D. Wang, Y. Bunimovich, A. Boukai, J. R. Heath, *Small* **2007**, *3*, 2043.
[4] I. Gur, N. A. Fromer, C. P. Chen, A. G. Kanaras, A. P. Alivisatos, *Nano Lett.* **2007**, *7*, 409.
[5] D. Wang, C. M. Lieber, *Nat. Mater.* **2003**, *2*, 355.
[6] S. P. Murarka, D. B. Fraser, A. K. Sinha, H. J. Levinstein, *IEEE Trans. Electron Devices* **1980**, *27*, 1409.
[7] J. Chen, J. P. Colinge, D. Flandre, R. Gillon, J. P. Raskin, D. Vanhoenacker, *J. Electrochem. Soc.* **1997**, *144*, 2437.
[8] P. Ritterskamp, A. Kuklya, M.-A. W. Stkamp, K. Kerpen, C. Weidenthaler, M. Demuth, *Angew. Chem.* **2007**, *119*, 7917; *Angew. Chem. Int. Ed.* **2007**, *46*, 7770.
[9] Y. N. Xia, P. D. Yang, Y. G. Sun, Y. Y. Wu, B. Mayers, B. Gates, Y. D. Yin, F. Kim, Y. Q. Yan, *Adv. Mater.* **2003**, *15*, 353.
[10] C. M. Lieber, *MRS Bull.* **2003**, *28*, 486.
[11] P. Gao, Z. L. Wang, *J. Phys. Chem. B* **2002**, *106*, 12653.
[12] J. Y. Lao, J. G. Wen, Z. F. Ren, *Nano Lett.* **2002**, *2*, 1287.
[13] A. G. Kanaras, C. Sonnichsen, H. T. Liu, A. P. Alivisatos, *Nano Lett.* **2005**, *5*, 2164.
[14] M. J. Bierman, Y. K. A. Lau, A. V. Kvit, A. L. Schmitt, S. Jin, *Science* **2008**, *320*, 1060.
[15] H. Yan, R. He, J. Johnson, M. Law, R. J. Saykally, P. Yang, *J. Am. Chem. Soc.* **2003**, *125*, 4728.
[16] S. Pavasupree, S. Ngamsinlapasathian, Y. Suzuki, S. Yoshikawa, *J. Nanosci. Nanotechnol.* **2006**, *6*, 3685.
[17] C. W. Peng, T. Y. Ke, L. Brohan, M. Richard-Plouet, J. C. Huang, E. Puzenat, H. T. Chiu, C. Y. Lee, *Chem. Mater.* **2008**, *20*, 2426.
[18] Z. W. Pan, Z. R. Dai, Z. L. Wang, *Science* **2001**, *291*, 1947.
[19] E. I. Givargizov, *J. Cryst. Growth* **1975**, *31*, 20.
[20] T. Wang, S.-Y. Oh, W.-J. Lee, Y.-J. Kim, H.-D. Lee, *Appl. Surf. Sci.* **2006**, *252*, 4943.
[21] B. Xiang, Q. X. Wang, Z. Wang, X. Z. Zhang, L. Q. Liu, J. Xu, D. P. Yu, *Appl. Phys. Lett.* **2005**, *86*.
[22] S. Zhou, X. H. Liu, Y. J. Lin, D. W. Wang, unpublished results.
[23] J. Du, P. Y. Du, P. Hao, Y. F. Huang, Z. D. Ren, G. R. Han, W. J. Weng, G. L. Zhao, *J. Phys. Chem. C* **2007**, *111*, 10814.
[24] J. Hyeongtag, C. A. Sukow, J. W. Honeycutt, G. A. Rozgonyi, R. J. Nemanich, *J. Appl. Phys.* **1992**, *71*, 4269.
[25] F. Meinardi, L. Moro, A. Sabbadini, G. Queirolo, *Europhys. Lett.* **1998**, *44*, 57.
[26] G. L. Kenneth, *Rep. Prog. Phys.* **2005**, *68*, 855.
[27] C. J. Kim, K. Kang, Y. S. Woo, K. G. Ryu, H. Moon, J. M. Kim, D. S. Zan, M. H. Jo, *Adv. Mater.* **2007**, *19*, 3637.
[28] A. L. Schmitt, L. Zhu, D. Schmeisser, F. J. Himpsel, S. Jin, *J. Phys. Chem. B* **2006**, *110*, 18142.
[29] R. Beyers, R. Sinclair, *J. Appl. Phys.* **1985**, *57*, 5240.
[30] M. Ekman, V. Ozolins, *Phys. Rev. B* **1998**, *57*, 4419.

